

Ultracold Rb-OH Collisions and Prospects for Sympathetic Cooling

Manuel Lara,¹ John L. Bohn,¹ Daniel Potter,² Pavel Soldán,³ and Jeremy M. Hutson²

¹*JILA, NIST, and Department of Physics, University of Colorado, Boulder, Colorado 80309-0440, USA*

²*Department of Chemistry, University of Durham, South Road, Durham, DH1 3LE, United Kingdom*

³*Doppler Institute, Department of Physics, Faculty of Nuclear Sciences and Physical Engineering, Czech Technical University, Břehová 7, 115 19 Praha 1, Czech Republic*

(Received 5 July 2006; published 3 November 2006)

We compute *ab initio* cross sections for cold collisions of Rb atoms with OH radicals. We predict collision rate constants of order 10^{-11} cm³/s at temperatures in the range 10–100 mK at which molecules have already been produced. However, we also find that in these collisions the molecules have a strong propensity for changing their internal state, which could make sympathetic cooling of OH in a Rb buffer gas problematic in magnetostatic or electrostatic traps.

DOI: [10.1103/PhysRevLett.97.183201](https://doi.org/10.1103/PhysRevLett.97.183201)

PACS numbers: 33.80.Ps, 34.20.Mq, 34.50.-s

A great way to make something cold is to place it in thermal contact with something else even colder. Thus, for many years, it has been possible to cool one species of ion sympathetically, by placing it in contact with another species that is being actively cooled [1,2]. More recently, ultracold neutral atoms have also been sympathetically cooled [3]. At slightly higher temperatures, atoms and molecules have been sympathetically cooled in a helium buffer gas [4]. Molecules are widely regarded as worth cooling to ultralow temperatures (typically around 1 μ K), where de Broglie wavelengths become large, and intermolecular interactions are dominated by long-range forces. Under such circumstances, the possibility of permanent electric dipole moments is expected to lead to novelties in such areas as precision measurement, collisions and chemistry, quantum degenerate matter, and quantum information theory [5].

A host of molecular cooling techniques have been proposed [5], but two that stand out are buffer-gas cooling (BGC), in which the cold He gas cools the molecules, and Stark deceleration (SD), in which polar molecules are slowed by carefully designed time-varying electric fields [6]. These techniques tend to produce “lukewarm” gases, with translational temperatures in the 10–100 mK range. They are therefore somewhat at a disadvantage with respect to the direct production of molecules by photoassociation from a gas of ultracold atoms [7]. Nevertheless, BGC and SD are extremely appealing for the far greater variety of molecular species that they can cool.

In this Letter we are concerned with the possibility of turning a 10 mK gas of molecules into a 10 μ K gas, by sympathetically cooling with Rb. For this cooling to be effective, the cross sections must be favorable. Namely, elastic scattering should occur frequently (with large cross sections σ_{el}), to make the necessary thermal contact. On the other hand, inelastic collisions that change the state of the molecules should occur infrequently (with small cross sections σ_{inel}). This is because either magnetostatic or electrostatic trapping demands that the molecules remain in a well-defined internal state. Until now, cross sections

for *m*-level-changing cold collisions of alkali atoms with molecules were wholly unknown. In this Letter we present the first such collision results, using a set of complete *ab initio* potential energy surfaces (PESs), and incorporating the hyperfine structure of the collision partners.

Our prototype system for this study consists of OH molecules in a bath of Rb atoms. This is a particularly timely example: the OH radical has been successfully slowed by Stark deceleration techniques in at least two laboratories, which can now produce ~ 10 mK packets of these molecules on demand [6,8]. At the same time, Rb is easily cooled and trapped in copious quantities at tens or hundreds of μ K, making it an ideal target for the molecules. In addition, the Rb-OH collision system is subject to a “harpooning” process, similar to that in Rb-NH [9], where during a collision the valence electron jumps from Rb to OH [10]. This process is without precedent in the cold collisions literature. Thus, even apart from sympathetic cooling, the Rb-OH scattering system is quite rich from a cold collisions perspective.

We begin by describing the potential energy surfaces (PES’s) of the system, as functions of (R, θ) , where R is the distance between the atom and diatom, and θ is the angle that the Jacobi vector \vec{R} makes with the OH axis. The OH monomer has a $^2\Pi$ ground state arising from a π^3 configuration, while the ground state of Rb is 2S . This produces $^1\Pi$ and $^3\Pi$ states for linear RbOH, which split into $^1A'$, $^1A''$ and $^3A'$, $^3A''$ surfaces at nonlinear geometries. We will refer to these as the covalent states. In addition, RbOH has an ion-pair state analogous to the ones previously found for RbNH [9]. The ion-pair threshold for $\text{Rb}^+ (^1S) + \text{OH}^- (^1\Sigma^+)$ lies only 2.35 eV above the ground state at $R = \infty$ and produces a $^1\Sigma^+ (^1A')$ state that cuts steeply down, crossing the covalent states near 6 Å. This is an actual crossing at linear geometries, where the ion-pair and covalent states have different symmetries, but there are avoided crossings between the two states of $^1A'$ symmetry at nonlinear geometries. There is therefore a conical intersection between the two $^1A'$ surfaces at linear geometries.

Potential energy surfaces for all 5 electronic states of RbOH were calculated by complete active space self-consistent field (CASSCF) calculations followed by multi-reference configuration interaction (MRCI). A full description will be given elsewhere [11]. All calculations used the MOLPRO package [12], with aug-cc-pVTZ basis sets [13] in uncontracted form for O and H and the ECP28MWB small-core quasirelativistic effective core potential [14] for Rb, with the valence basis set from Ref. [15]. The CASSCF calculation included all configurations that can be formed from the lowest (10, 3) orbitals of (a' , a'') symmetry, with the lowest (5, 1) orbitals doubly occupied. Energies were calculated in Jacobi coordinates (R , θ) on a grid of 25 unequally spaced points in R from 2 to 12 Å and 11 Gauss-Lobatto quadrature points in θ . The two $^1A'$ surfaces were transformed to obtain two quasidiabatic diagonal surfaces and a coupling surface, using a mixing angle derived from matrix elements of the OH \hat{L}_z operator. Finally, the quasidiabatic covalent energies were extrapolated to $R = \infty$ using C_6 and C_7 coefficients obtained from coupled cluster (CCSD) calculations at $R = 15, 25$, and 100 Å. The singlet and triplet sum and difference surfaces were expanded in normalized associated Legendre functions and the radial coefficients were interpolated using the reciprocal-power reproducing kernel Hilbert space (RP-RKHS) method [16,17].

The resulting diabatic covalent surfaces have wells 337 and 511 cm^{-1} deep at linear Rb-OH geometries for the singlet and triplet surfaces, respectively. For the A' surfaces this linear well is the absolute minimum, but the A'' surfaces have absolute minima at nonlinear geometries ($\theta \approx 125^\circ$) with depths of 405 and 615 cm^{-1} , respectively. The ion-pair state is very much deeper, with a well $\sim 26000 \text{ cm}^{-1}$ below the neutral threshold.

To perform scattering calculations on these surfaces, we expand the wave function into an appropriate basis set consisting of the quantum numbers of the atom and diatom in the separated limit. For the atom, electronic (s_a) and nuclear (i_a) spins are coupled to make total spin $|f_a m_{f_a}\rangle$ in the lab frame. For the diatom, the electronic wave function is specified in Hund's coupling case (a) by the total electronic angular momentum j , with projections m_j in the lab frame and ω in the frame rotating with the molecule. As usual, ω is separated into its orbital and spin components, $\omega = \lambda + \sigma$. Linear combinations $|\bar{\lambda} \bar{\omega} \epsilon\rangle = (|\lambda \omega\rangle + \epsilon|-\lambda - \omega\rangle)/\sqrt{2}$ are constructed to produce states of good parity appropriate to the zero-electric-field case we consider here. Finally, j is coupled to the nuclear spin i_d of the hydrogen atom to yield total diatom spin $|f_d m_{f_d}\rangle$. The partial wave quantum numbers $|LM_L\rangle$ account for the relative orientation of the collision pair in the lab frame. Thus the basis states of our calculation are given by

$$|s_d \bar{\lambda} \bar{\omega} \epsilon(j i_d) f_d m_{f_d}\rangle |s_a i_a\rangle |f_a m_{f_a}\rangle |LM_L\rangle. \quad (1)$$

In this basis the total parity $p = \epsilon(-1)^{j-s_d+L}$ and the lab projection of total angular momentum, $m_{f_d} + m_{f_a} + M_L$,

are conserved quantities. In zero field, the total angular momentum $\mathcal{F} = \mathbf{f}_d + \mathbf{f}_a + \mathbf{L}$ would also be conserved; however, we anticipate considering the action of a field on the collisions, which would mix different \mathcal{F} values. We therefore do not exploit this symmetry here.

Cast in this basis, the Schrödinger equation for Rb-OH collisions takes the standard form of a set of close-coupled equations in the variable R . To solve these, we propagate the log-derivative matrix $Y \equiv d\psi/dR\psi^{-1}$ using a variable-step version of Johnson's algorithm [18]. Because of the multiple PESs and the inclusion of hyperfine degrees of freedom, the total number of scattering channels required to solve the complete problem including spin (in excess of 25 000) is prohibitively large.

To overcome this obstacle, we exploit a kind of frame-transformation procedure [19]. We identify a suitable radius $R = R_0$, and define $R < R_0$ and $R > R_0$ as the "short-range" and "long-range" parts of the calculation, respectively. For Rb-OH, we choose $R_0 = 17a_0$. In the short-range region, the PES's are deep, and the hyperfine effects are small. We therefore compute Y in a basis of decoupled nuclear spins and neglect couplings between blocks of the Hamiltonian with different nuclear spin projections m_{i_a} or m_{i_d} . In this pilot study, we have neglected the influence of the ion-pair channel.

At long range, $R > R_0$, the full hyperfine structure is restored, and Y is transformed into the basis (1) for further propagation and matching to spherical Bessel functions to yield scattering matrices. In this region, collision channels in which the molecule is excited into higher-lying rotational or spin-orbit states are already strongly closed. We therefore eliminate these channels. In the inner region, we use partial waves up to $L = 28$ and rotational states up to $j = 11/2$. In the outer region, we employ partial waves up to $L = 22$, but with full hyperfine structure of the $j = 3/2$ rotational ground state. Because of these approximations, no single calculation requires more than 2000 channels [11]. Numerical checks suggest that the magnitudes of cross sections computed in this way are accurate to within a factor of ~ 2 .

For concreteness, we calculate cross sections for a beam experiment in which the incident wave vector is coincident with the laboratory quantization axis. Energy-dependent cross sections for two different initial states of the collision partners are shown in Fig. 1. In the first case, Fig. 1(a), the Rb atom is initially in its "stretched" state, with $|f_a m_{f_a}\rangle = |22\rangle$, and the molecule is in its higher-lying, f parity state, and also spin stretched, with $|f_d m_{f_d}\rangle = |22\rangle$. Both these states are weak-magnetic-field seeking, meaning that they can be trapped magnetically. In addition, OH in this state can be trapped electrostatically. Solid lines denote elastic cross sections σ_{el} , in which all internal quantum numbers are retained after the collision, and dashed lines refer to inelastic cross sections σ_{inel} , which represents the sum of state-to-state cross sections to many possible outcomes distinct from the initial channel (including m_{f_a} and

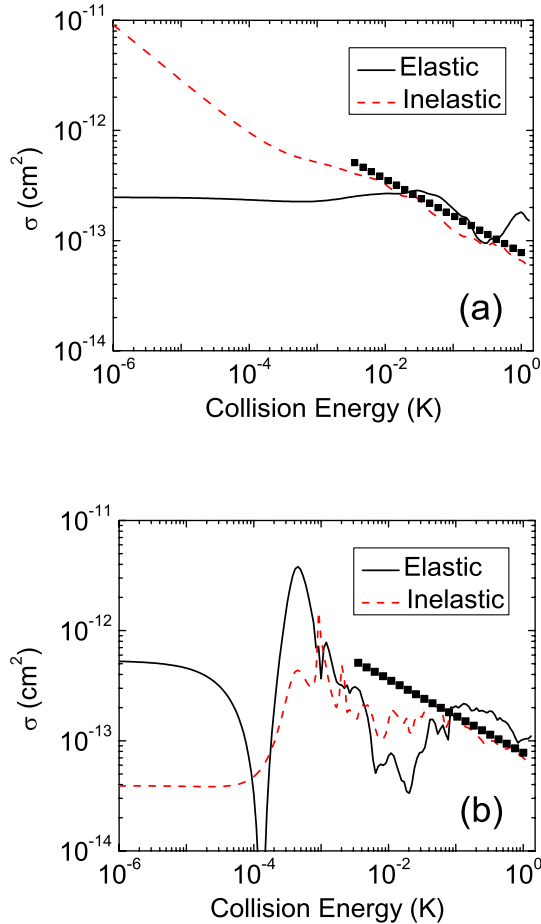


FIG. 1 (color online). Rb-OH collision cross sections vs energy. Solid (dashed) lines represent elastic (inelastic) cross sections. In (a) results are shown for the incident channel $|^2\Pi_{3/2}, f_d m_{f_d} = 22, f\rangle_{\text{OH}} |f_a m_{f_a} = 22\rangle_{\text{Rb}}$, where both the atom and diatom are weak-magnetic-field seeking, and the OH is also weak-electric-field seeking. In (b) the incident channel is shown $|^2\Pi_{3/2}, f_d m_{f_d} = 11, e\rangle_{\text{OH}} |f_a m_{f_a} = 1 - 1\rangle_{\text{Rb}}$. Again, both species are in weak-magnetic-field seeking states, but the OH is now in a strong-electric-field seeking state. The points indicate the Langevin cross section, Eq. (2).

m_j -changing collisions that do not release energy at zero field).

The results in Fig. 1 clearly demonstrate that σ_{inel} is often equal to, or greater than, σ_{el} over much of the energy range. That this should be so can be seen qualitatively by considering the flow of angular momentum during a collision. The total angular momentum projection $M_{\mathcal{F}} = m_{f_a} + m_{f_d} + M_L$ is conserved, where $m_{f_d} = m_j + m_{i_d} = m_n + m_{s_d} + m_{i_d}$ contains the spin-independent projection m_n . In the absence of anisotropy in the potential energy surface, m_n and M_L would be separately conserved, and therefore m_{f_a} and m_{f_d} would be conserved in stretched states. However, the anisotropy allows m_n to change readily, hence changing the overall projection of the diatom's angular momentum. Moreover, the fact that OH is a Hund's

case (a) molecule means that m_n and m_{s_d} are not separate entities so that the electronic spin projection is also changed in a collision. The general view is one of a complete “scrambling” of the internal degrees of freedom of the OH molecule upon colliding with Rb; this picture is substantiated by partial cross sections, which show significant scattering into all channels that are allowed by energy and angular momentum conservation [11].

At low energies, the cross sections in Fig. 1(a) vary in accordance with the Wigner law, with σ_{el} constant at threshold, and $\sigma_{\text{inel}} \propto 1/\sqrt{E}$. At higher energies, the inelastic cross section can be roughly estimated by exploiting the idea that the internal state of the molecule is completely disrupted during a collision. Such a process can be approximated simply by a Langevin model [10]: for a given energy E , there is a maximum partial wave $L(E)$ for which E lies above the centrifugal barrier of the long-range potential $-C_6/R^6 + \hbar^2 L(L+1)/2\mu R^2$. Here $C_6 = 325E_h a_0^6$ is the isotropic van der Waals coefficient of the PES [11], and μ the reduced mass of the collision pair. In the Langevin model, we assume that any partial wave smaller than $L(E)$ contributes to inelastic scattering with unit probability, i.e., any time the atom and molecule are near one another, their internal states are always disrupted. This idea leads to a cross section

$$\sigma_{\text{Langevin}}(E) = 3\pi \left(\frac{C_6}{4E} \right)^{1/3}. \quad (2)$$

This cross section is also shown in Fig. 1(a), by the solid symbols. It is clearly getting the trend and the order of magnitude of the cross sections correct.

In this pilot calculation, we have not included the effect of the ion-pair channel. However, in light of the near-complete disruption of molecular state already included in the model, including the ion-pair channels would likely only disrupt the internal states more severely, and would not change this basic conclusion about sympathetic cooling. Preliminary calculations have indeed found this to be the case [11]. Note that our cross sections are already larger than the geometric cross section $\sigma = 4\pi R_0^2 = 4.5 \times 10^{-14} \text{ cm}^2$ for a crossing radius $R_0 = 6 \text{ \AA}$.

We turn now to an alternative pair of initial states, whose scattering cross sections are shown in Fig. 1(b). Here the atom is in its lowest magnetically trappable state, with $|f_a m_{f_a}\rangle = |1 - 1\rangle$, and the molecule is in its lower-energy e state, with total spin $|f_d m_{f_d}\rangle = |11\rangle$ (also magnetically trappable). At zero field, both σ_{el} and σ_{inel} are energy-independent at low energies, since all exit channels are isoenergetic with the incident channel. In nonzero field, the $|11\rangle_{\text{OH}} |1 - 1\rangle_{\text{Rb}}$ channel lies above other m components in energy, and σ_{inel} would again diverge.

By the same token, sympathetic cooling is possible at low energies for OH molecules in the $|1 - 1\rangle$ state and Rb atoms in the $|11\rangle$ state. This is the lowest-energy channel of all: there are no inelastic channels energetically available and σ_{inel} will vanish. These states are not magnetically

trappable, but could be confined in an optical or microwave [20] dipole trap or an alternating current trap [21]. A small static magnetic field will be needed to maintain the projection quantum numbers.

At higher collision energies, other forms of inelastic scattering become energetically allowed. Once the collision energy surpasses the height of the p -wave centrifugal barrier (at about 1.6 mK), the molecule can shed angular momentum into the partial wave degree of freedom. At this point σ_{inel} climbs to a large value, comparable to σ_{el} . Further, at about 4 mK, the $f = 2$ hyperfine state of OH becomes energetically allowed, providing another route to inelastic collisions. By examining the partial cross sections, we find that these two avenues for inelastic collisions are roughly equally likely. At still higher collision energies, σ_{inel} is again roughly approximated by the Langevin result (2), although there is now more structure, owing to a large number of Feshbach resonances to fine and hyperfine excited states.

These results present a cautionary tale for sympathetic cooling using alkali atoms. One may regard inelastic scattering as a “Murphy’s Law” process [22]. Namely, if the internal state of the molecule can change to produce an unfavorable result, it will do so. The key to making sympathetic cooling viable lies in eliminating undesirable channels as far as possible. For example, a light collision partner with a small C_6 coefficient will produce a centrifugal barrier at higher energy, preventing partial waves from accepting angular momentum. This circumstance explains, at least partly, the ability of a He buffer gas to cool molecules without badly disrupting spin orientation [23–25]. In the present context of alkali atoms, consider Li, which is about 12 times lighter than Rb, and about half as polarizable. Its p -wave centrifugal barrier upon colliding with OH is on the order of 10 mK. In addition, a molecule that is better described by Hund’s coupling case (b), in which the electron’s spin is only weakly coupled to the molecular rotation axis, may help weaken σ_{inel} below the Langevin limit [25].

In summary, we have performed the first *ab initio* scattering calculations for an open-shell, ground state molecule colliding with an alkali atom, incorporating the hyperfine structure of both collision partners. The results suggest that elastic cross sections are sufficiently large for sympathetic cooling to occur, yet equally large inelastic cross sections probably hinder this application. Nonetheless, the results do not preclude the possibility that, by applying electric or magnetic fields, inelastic cross sections could be suppressed [26,27]. This will be the subject of a future study.

M. L. and J. L. B. gratefully acknowledge the NSF and the W. M. Keck Foundation. P. S. acknowledges the MŠMT CR (Grant No. LC06002).

-
- [1] R. E. Drullinger *et al.*, Applied Physics (Berlin) **22**, 365 (1980).
 - [2] D. J. Larson *et al.*, Phys. Rev. Lett. **57**, 70 (1986).
 - [3] This was first reported by C. J. Myatt *et al.*, Phys. Rev. Lett. **78**, 586 (1997).
 - [4] R. deCarvalho *et al.*, Eur. Phys. J. D **7**, 289 (1999).
 - [5] Special issue on cold molecules, edited by J. Doyle, B. Friedrich, R. V. Krems, and F. Masnou-Seeuws [Eur. Phys. J. D **31**, 149 (2004)], and references therein.
 - [6] S. Y. T. van de Meerakker, N. Vanhaecke, and G. Meijer, Annu. Rev. Phys. Chem. **57**, 159 (2006).
 - [7] K. M. Jones, E. Tiesinga, P. D. Lett, and P. S. Julienne, Rev. Mod. Phys. **78**, 483 (2006).
 - [8] J. R. Bochinski, E. R. Hudson, H. J. Lewandowski, and J. Ye, Phys. Rev. A **70**, 043410 (2004).
 - [9] P. Soldán and J. M. Hutson, Phys. Rev. Lett. **92**, 163202 (2004).
 - [10] R. D. Levine and R. B. Bernstein, *Molecular Reaction Dynamics and Chemical Reactivity* (Oxford, New York, 1987).
 - [11] M. Lara *et al.* (to be published).
 - [12] H.-J. Werner, P. J. Knowles, R. Lindh, M. Schütz *et al.*, MOLPRO quantum chemistry package, version 2002.6, 2002; <http://www.molpro.net/>.
 - [13] T. H. Dunning, Jr., J. Chem. Phys. **90**, 1007 (1989).
 - [14] T. Leininger *et al.*, Chem. Phys. Lett. **255**, 274 (1996).
 - [15] P. Soldán, M. T. Cvitaš, and J. M. Hutson, Phys. Rev. A **67**, 054702 (2003).
 - [16] T.-S. Ho and H. Rabitz, J. Chem. Phys. **104**, 2584 (1996).
 - [17] P. Soldán and J. M. Hutson, J. Chem. Phys. **112**, 4415 (2000).
 - [18] B. R. Johnson, J. Comput. Phys. **13**, 445 (1973).
 - [19] U. Fano and A. R. P. Rau, *Atomic Collisions and Spectra* (Academic, New York, 1986).
 - [20] D. DeMille, D. R. Glenn, and J. Petricka, Eur. Phys. J. D **31**, 375 (2004).
 - [21] J. van Veldhoven, H. L. Bethlem, and G. Meijer, Phys. Rev. Lett. **94**, 083001 (2005).
 - [22] R. A. J. Matthews, Proceedings of the Royal Institution of Great Britain **70**, 75 (1997).
 - [23] J. D. Weinstein *et al.*, Nature (London) **395**, 148 (1998).
 - [24] J. L. Bohn, Phys. Rev. A **61**, 040702 (2000); **62**, 032701 (2000).
 - [25] R. V. Krems, A. Dalgarno, N. Balakrishnan, and G. C. Groenenboom, Phys. Rev. A **67**, 060703 (2003).
 - [26] C. Ticknor and J. L. Bohn, Phys. Rev. A **71**, 022709 (2005).
 - [27] R. V. Krems, Int. Rev. Phys. Chem. **24**, 99 (2005).